Energy 36 (2011) 3878–3887

Contents lists available at ScienceDirect

Energy

journal homepage: www.elsevier.com/locate/energy

Thermoeconomic analysis of a low-temperature multi-effect thermal desalination system coupled with an absorption heat pump

Yongqing Wang [a,*], Noam Lior [b]

[a] Cleaning Combustion and Energy Utilization Research Center of Fujian Province, Jimei University, Xiamen 361021, PR China
[b] Department of Mechanical Engineering and Applied Mechanics, University of Pennsylvania, Philadelphia, PA 19104-6315, USA

ARTICLE INFO

Article history:
Received 25 February 2010
Received in revised form
25 August 2010
Accepted 7 September 2010
Available online 4 November 2010

Keywords:
Water desalination
Multi-effect evaporation water desalination
Absorption heat pumps
Ejector heat pumps
Thermodynamic performance
Economic performance

ABSTRACT

This study presents a thermal and economic performance analysis of a LT-MEE (low-temperature multi-effect evaporation) water desalination system coupled with an LiBr–H_2O ABHP (absorption heat pump). A 60–78% water production increase over a stand-alone LT-MEE run at the same heat source conditions can be obtained owing to the coupling. A detailed thermodynamic sensitivity analysis of the ABHP-MEE is performed. Although ABHP is usually considered to be more efficient than an EHP (ejector heat pump), we also compare the thermal performance of the ABHP-MEE with an integrated EHP-MEE system. The results show that the ABHP has a more favorable thermal performance than the EHP only in certain parameters ranges. The reasons and these parameters ranges are discussed. The economic analysis of the ABHP-MEE shows that the capital cost of the ABHP accounts for a very small part of the water cost, and when designing an ABHP for an existing MEE unit, the parameters selection of an ABHP for lower water cost is consistent with that for better thermal performance. The unit steam cost is an important factor in determining whether the ABHP-MEE or the EHP-MEE is economically favorable, with the influence discussed. Also, a recommended general procedure for economic comparison between ABHP-MEE and EHP-MEE is outlined.

1. Introduction

LT-MEE (Low-temperature multi-effect evaporation) water desalination is attractive, and indeed used in many installations, mainly because of low corrosion rate, power consumption and capital cost relative to the commonly used MSF (multi-stage flash) desalination process [1,2]. The top brine temperature of LT-MEE is usually lower than 70 °C, and correspondingly, the saturation temperature/pressure of the heating steam needed to run an LT-MEE is also low. For instance, Darwish and Alsairafi [2] described two sample units driven by steam with saturation temperatures of 60 °C and 65 °C, respectively.

When driving steam is available at higher pressures/temperatures than needed for the LT-MEE process, good potential exists for increasing fresh water production by combining the LT-MEE with heat pumps. Among the three types of thermally-driven heat pumps – EHP (ejector heat pumps), ABHP (absorption heat pumps) and ADHP (adsorption heat pumps), the ADHP is relatively new and not as technically mature as the former two, so its coupling with desalination will not be discussed here.

Systems combining EHP and LT-MEE have been commercialized and built in many places, with significant increase of water production over stand-alone LT-MEE with the same driving heat source conditions, as shown in two cases [2,3], where the water production increased by about 67% and 77%, respectively, owing to the coupling with EHP.

The combined systems of ABHP with thermal desalination have been studied by many researchers, and some of the studies focusing on the ABHP-MEE systems are: Aly [4] proposed a configuration composed of a single-effect LiBr–H_2O ABHP and a 20-effect LT-MEE with an evaporation temperature range of 6–63 °C, and predicted a performance ratio (defined as the mass ratio of the produced water and the motive steam) of 14.2 with a by-product of cooling capacity; Su et al. [5] studied a system consisted of a double-effect LiBr–H_2O ABHP and a 9-effect LT-MEE, obtaining a performance ratio of 17.15, much higher than the 11.05 of an EHP-MEE system; Gunzbourg and Larger [6] proposed a power and water cogeneration system, which is the combination of a gas turbine power plant, an ABHP, and a 14-effect MEE with top brine temperature of 74 °C; Alarcon-Padilla et al. [7] described a double-effect ABHP-operated MEE system demonstrated in Spain, with a performance ratio of 21.3 compared with that of 10 for a stand-alone MEE unit. The literature shows that coupling of ABHP with desalination was

* Corresponding author. Tel.: +86 592 6180597; fax: +86 592 6183523.
E-mail address: yongqing@jmu.edu.cn (Y. Wang).

0360-5442/$ – see front matter © 2010 Elsevier Ltd. All rights reserved.
doi:10.1016/j.energy.2010.09.028

Nomenclature

c	unit water cost of ABHP-MEE, $/ton
C	capital cost, $
COP	coefficient of performance
D	water production capacity, ton/day
E	thermal exergy [kW]
f	plant availability factor
h	specific enthalpy [kJ/kg]
i	interest rate
m	mass flow rate [kg/s]
n	number of life year
N	payback period, y
p	pressure [MPa]
Q	thermal energy [kW]
r	performance ratio
s	specific entropy [kJ/kg K]
T	temperature [K, °C]
w_{min}	specific work needed in an ideal separation process [kJ/kg]
w_P	specific mechanical work needed in desalination process [kJ/kg]
X	mass concentration of LiBr solution [%]
y	unit steam cost, $/ton
Y	annual cost, $/y
Y_{ABHP}	annual cost increased by adding ABHP, $/y
Y_s	annual thermal energy cost saved by ABHP-MEE comparing with EHP-MEE, $/y
Z	annual capital and operating cost (excluding thermal energy cost) of MEE, $/y
α	amortization factor
ϵ	exergy efficiency [%]
λ_R	non-dimensional exergy recovery parameter [%]
ξ	non-dimensional exergy destruction parameter [%]

Abbreviations

ABHP	absorption heat pump
ADHP	adsorption heat pump
EHP	ejector heat pump
LT	low-temperature
MEE	multi-effect evaporation
MSF	multi-stage flash

Subscripts

A	absorber
d	destruction
D	desalination
f	feed seawater
G	generator
hp	heat pump
i	effect i
in	input
min	minimum
max	maximum
others	components except absorber and generator in absorption subsystem
R	recovery
sat	saturation
SH	solution heat exchanger
sup	superheat
v	vapor
0	base case, ambient
1, 2, …	states on the system flow sheet

investigated only theoretically, and to the authors' knowledge, the only test facility is the one demonstrated in Spain [7].

The main objective of the paper is to investigate the thermal and economic performance of a system combined of a single-effect LiBr–H_2O ABHP and an LT-MEE, to improve the understanding of the system, and of ways to improve and optimize it. Although ABHP is usually considered to be more efficient than EHP, as partially verified by several studies [5,7], we also compare the performance of integrating an LT-MEE system with an EHP, to clarify the conditions at which ABHP is advantageous over EHP in desalination processes. Our results show that ABHP-MEE has more favorable thermal and economic performance than EHP-MEE in only certain parameter ranges, and the reasons and parameters are discussed.

2. System configuration

Fig. 1 schematically shows an ABHP-MEE system. Line B–B divides the configuration into two interconnected parts: left to B–B is the absorption subsystem and right to B–B is the MEE subsystem. The heating steam (15) for the MEE comes from three sources: one (13) is the water boiled off from the ABHP generator G by the motive steam (1) that heats the LiBr–H_2O mixture in it; another (12) is from the absorber A, where part of the vapor (10) produced in the last effect of MEE is absorbed and the absorption heat is used to heat and vaporize part of the condensate (11) from the first-effect evaporator E_1; and the third one (14) is from the flash chamber FC, where a small amount of steam flashes off the motive steam condensation (2). Detailed description of the working process of MEE can be found in many publications (cf. [2,8]).

3. Thermodynamic performance criteria used and thermodynamic sensitivity analysis of the ABHP-MEE system

3.1. Thermodynamic performance criteria

For thermodynamic performance evaluation we define the exergy efficiency ε, which is the ratio of the minimal work needed for producing fresh water from seawater by a reversible separation process, and the exergy needed in a real process with the same amount of product:

$$\varepsilon = \frac{W_{min}}{E_{in} + W_P} = \frac{m_{17} W_{min}}{m_1[h_1 - h_3 - T_0(s_1 - s_3)] + m_{17} W_P} \quad (1)$$

where E_{in} is the thermal exergy input into the system, and W_P and W_{min} represent the mechanical work consumed in a real desalination process and the minimum work needed in a reversible separation process, respectively, for producing 1 kg fresh water. The calculation method of W_{min} was given by Wang and Lior [9].

Performance ratio r, which is the mass ratio of the produced water and the motive steam,

$$r = m_{17}/m_1 \quad (2)$$

is the most commonly used criterion for performance evaluation of thermal desalination systems. Applicable only to thermal performance comparison of the desalination systems driven by the same heat source conditions, r is not a performance criterion as reasonable thermodynamically as the exergy efficiency defined above. Nevertheless, r is also calculated in this paper for reference.

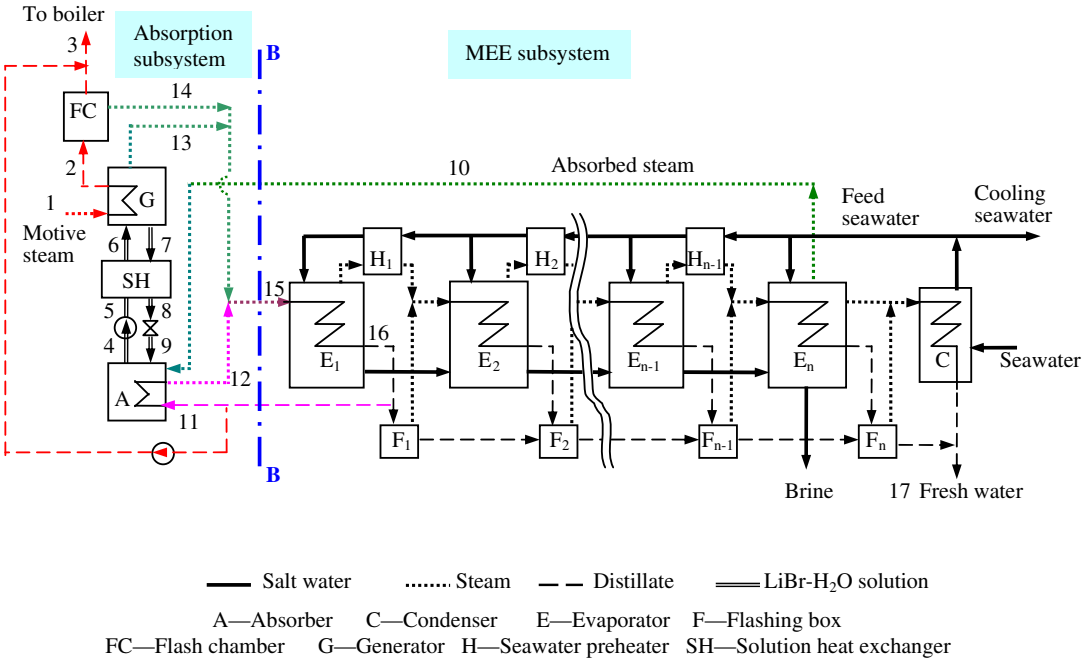

Fig. 1. Schematic diagram of the ABHP-MEE system considered in this study.

A dimensionless exergy destruction parameter, ξ, is used to evaluate the overall thermodynamic irreversibility of the processes occurred in each component:

$$\xi = \frac{E_d}{E_{\text{in}} + W_P} = \frac{E_d}{m_1[h_1 - h_3 - T_0(s_1 - s_3)] + m_{17}W_P} \tag{3}$$

where E_d represents the process exergy destruction. Part of the vapor produced in the last effect of MEE is entrained to the absorber and its exergy, E_R, is recovered. The dimensionless exergy recovery parameter is defined as

$$\lambda_R = \frac{E_R}{E_{\text{in}} + W_P} = \frac{m_{10}[h_{10} - h_0 - T_0(s_{10} - s_0)]}{m_1[h_1 - h_3 - T_0(s_1 - s_3)] + m_{17}W_P} \tag{4}$$

Comparing the configuration of the ABHP-MEE system with that of the reference ABHP system (Fig. 2), we note that the first evaporator E_1 of the MEE serves as the condenser CN of the ABHP, and the evaporators E_1–E_n together play the role of the throttling valve V and the evaporator EA, so in a broad sense, the ABHP-MEE system can be regarded as a heat pump, of which the output is the thermal energy (exergy), Q_D (E_D), released by the heating steam (stream 15 in Fig. 1) in E_1, and the performance criteria — the coefficient of performance COP_{hp} and exergy efficiency ε_{hp} are defined as

$$COP_{\text{hp}} = \frac{Q_D}{Q_{in}} = \frac{m_{15}(h_{15} - h_{16})}{m_1(h_1 - h_3)} \tag{5}$$

$$\varepsilon_{\text{hp}} = \frac{E_D}{E_{\text{in}}} = \frac{m_{15}[h_{15} - h_{16} - T_0(s_{15} - s_{16})]}{m_1[h_1 - h_3 - T_0(s_1 - s_3)]} \tag{6}$$

Similarly, the above discussion is also applicable to the EHP-MEE system (Fig. 3). When the performance of the MEE unit is specified, the water production of ABHP-MEE or EHP-MEE is up to Q_D (E_D). It is thus clear that COP_{hp} and ε_{hp} are criteria suitable for thermodynamic performance evaluation and comparison of EHP and ABHP in desalination processes.

To exhibit more clearly the sensitivity of water production, performance criteria such as ε, r, COP_{hp} and ε_{hp}, are normalized by their base-case values shown in Table 1 that also summarizes the main assumptions, parameters and thermodynamic performance of the base-case system. Referring to the operating conditions of an existing MEE unit [2], a six-effect MEE was chosen in the base-case calculation, and in accordance with industrial practice, all of the MEE evaporators were given the same heat transfer area [8].

The COP_{hp} of ABHP is 1.7 in the base case (Table 1), and 1.6–1.78 within the parameter ranges ($p_1 = 0.12$–0.5 MPa, $T_{16} = 56$–72 °C)

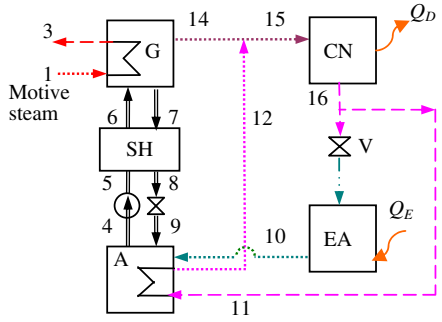

CN — Condenser EA — Evaporator V — Throttling valve
The other symbols are the same as in Fig. 1.

Fig. 2. Schematic diagram of the reference ABHP system.

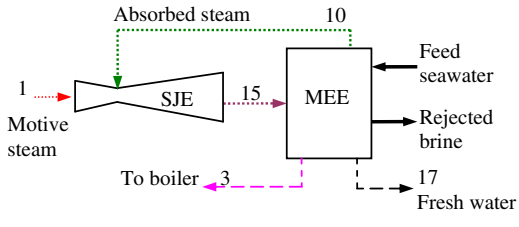

* SJE - steam jet ejector, and the other symbols are the same as in Fig. 1.

Fig. 3. Schematic diagram of an EHP-MEE system.

Table 1
Main assumptions, parameters and thermodynamic performance of the base-case ABHP-MEE system.

Main assumptions for the base-case calculation				
Ambient conditions (dead states for exergy analysis)				
Temperature				25 °C
Pressure				1 atm
Salinity of seawater				35,000 ppm
ABHP subsystem				
Mass flow of motive steam				1 kg/s
Pressure of motive steam (saturated), p_1				0.25 MPa
Generator approach temperature, ΔT_{1-7}				10 °C
Mass concentration difference between strong- and weak-solutions, ΔX				6%
Absorber approach temperature, ΔT_{4-12}				6 °C
Absorbed vapor pressure minus absorber operation pressure				40 Pa
Temperature difference at the cold side of solution heat exchanger, ΔT_{8-5}				10 °C
Minimum temperature difference between strong solution and crystallization point				15 °C
Maximum mass concentration of strong solution				65%
LT-MEE subsystem				
Number of effects				6
Salinity of the discharge brine				70,000 ppm
Salinity of produced fresh water				0
Temperature rise of seawater in preheater				4 °C
Condensation temperature of heating steam in the 1st effect, T_{16}				65 °C
Temperature difference at the hot side of end condenser C				4 °C
Saturation temperature of produced vapor in the last effect, $T_{10,sat}$				42 °C
Mechanical work consumption per kg produced fresh water				7.2 kJ [10]
Main parameters of the base-case system				
Absorption subsystem	T (℃)	p (kPa)	m (kg/s)	X (% LiBr)
Strong solution from generator G	117.4	25.02	6.92	61.7
Strong solution from heat exchanger SH	87.0	24.77	6.92	61.7
Weak solution from absorber A	77.0	8.17	7.66	55.7
Weak solution from heat exchanger SH	102.4	–	7.66	55.7
Steam produced (13) in generator G	110.4	25.02	0.745	0
Steam (stream 12 in Fig. 1) from absorber A	71.0	25.02	0.885	0
Steam (stream 14 in Fig. 1) from flashing chamber	65	25.02	0.112	0
LT-MEE subsystem	T_i (°C)	m_{fi} (kg/s)	m_{vi} (kg/s)	
Effect 1	62.2	3.49	1.74	
Effect 2	58.4	3.41	1.71	
Effect 3	54.5	3.34	1.67	
Effect 4	50.6	3.26	1.63	
Effect 5	46.7	3.18	1.59	
Effect 6	42.9	3.10	1.55	
Base-case performance				
Q_{D0}	4162 kW			
E_{D0}	494.4 kW			
COP_{hp0}	1.70			
ε_{hp0}	81.3%			
r_0	9.89			
ε_0	3.13%			

studied in the paper. Thus, owing to the coupling with the ABHP, the ABHP-MEE can produce 60–78% more water than a stand-alone LT-MEE unit run by the same heat source. The exergy efficiency ε_{hp} of the ABHP used in the desalination process, which is 81.3% in the base case, is much higher than that of the common ABHP systems. One of the main reasons for this improvement is that the energy (exergy) of the entrained steam (stream 10 in Fig. 1) is recovered, as discussed in Section 3.2.4.

3.2. Parametric analysis of the ABHP-MEE system

The simulation was carried out using the EES (Engineering Equation Solver) software [11]. The properties of LiBr–H_2O solution were from Kaita [12]; the properties of seawater and brine, the boiling point elevation of brine, as well as the non-equilibrium allowance of flashing evaporation in the flashing box were from El-Dessouky and Ettouney [8] and Husain [13]. The computerized models were validated by (1) checking the relative errors of mass and energy balance of each component and the entire system where they were found to be $<10^{-6}$, (2) comparing the simulation results of the ABHP unit and the LT-MEE unit separately with those in literature [3,14] under the same conditions where they show good agreement (for example, the relative errors of the coefficient of performance of the ABHP and the performance ratio of MEE are both within 3%).

Under the specified ambient conditions, the main factors influencing the thermodynamic performance of the ABHP-MEE system are the generator approach temperature ΔT_{1-7}, the LiBr–H_2O strong-and-weak solution concentration difference ΔX, the motive steam pressure p_1, the heating steam condensation temperature T_{16} in E_1 (or the generator operation pressure), and the entrained steam saturation temperature $T_{10,sat}$ (or the entrained steam pressure).

3.2.1. Influence of the generator approach temperature ΔT_{1-7}

Fig. 4 shows the normalized r and ε of the ABHP-MEE system for different generator approach temperature ΔT_{1-7} which is the temperature difference between the saturated motive steam and the generator exit strong solution. The other conditions are kept constant at the base-case values (Table 1) except those marked in the figure; this note is applicable to all the figures followed.

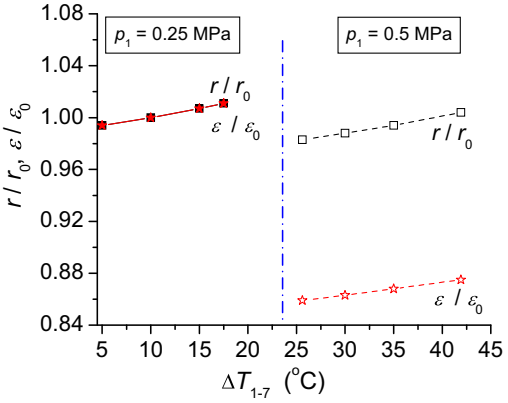

Fig. 4. Effect of the generator approach temperature ΔT_{1-7} on system performance.

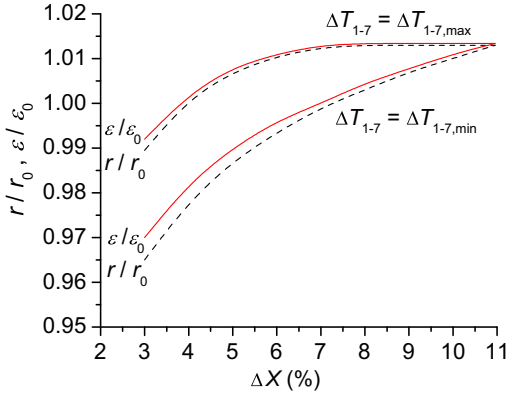

Fig. 5. Effects of ΔX on system performance.

Fig. 4 reveals that different input conditions generate different ranges of ΔT_{1-7}. For instance, the range of ΔT_{1-7} is 5 °C–17.5 °C when $p_1 = 0.25$ MPa, and 25.6 °C–41.9 °C when p_1 is changed to 0.5 MPa. $\Delta T_{1-7,min}$, the low limit of ΔT_{1-7}, is determined by two factors: one is the minimum ΔT_{1-7} technically allowed, which is taken as 5 °C [14] in this paper, and the other is the strong-solution crystallization temperature which rises with the decrease of ΔT_{1-7}. For specified p_1 and T_{16} and then specified T_1 and p_{13}, a lower ΔT_{1-7} raises T_7 and then raises X_7 for keeping a constant p_{13}, resulting in a higher crystallization temperature of the strong solution, thus making the solution more prone to crystallize and restricting the reduction of ΔT_{1-7}. The low limit of ΔT_{1-7} is the higher of the ΔT_{1-7} values determined by two limits, one determined by the minimal values needed for practical heat transfer and the other being the crystallization temperature. The increase of ΔT_{1-7} causes the operating temperature of the generator and then that of the absorber to decrease, thus decreasing the superheat temperature, ΔT_{sup}, of the heating steam (Stream 12 in Fig. 1) produced in the absorber (for instance, increasing ΔT_{1-7} from 5 °C to 10 °C under base-case conditions, leads to a decrease of ΔT_{sup} from 10 °C to 6 °C). When ΔT_{sup} reaches zero (that is, the heating steam is saturated), ΔT_{1-7} reaches the upper limit value, $\Delta T_{1-7,max}$.

The r and ε have a similar trend with the variation of ΔT_{1-7} (Fig. 4). For specified heat source conditions and then specified thermal exergy E_{in} input into the ABHP-MEE system, a higher r causes higher W_{min} and W_P [Eq. (1)]. Because the E_{in} accounts for the main part, say, higher than 90% [15], of the exergy consumed in the system, the numerator in Eq. (1) rises more steeply than the denominator, resulting in a higher ε.

As shown in Fig. 4, the r and ε of the ABHP-MEE increase with ΔT_{1-7}, and reaches the highest value under $\Delta T_{1-7,max}$. Our calculations show that for each 1 °C of increase in ΔT_{1-7}, the water production increases by about 0.12%–0.15%; increasing ΔT_{1-7} from the lowest to the upper limit, raises water production from 0 to more than 5%, depending on the calculation conditions input.

3.2.2. Influence of LiBr–H_2O strong-and-weak solution concentration difference ΔX

Fig. 5 shows the effect of the concentration difference, ΔX, between the strong and weak LiBr–H_2O solutions for $\Delta T_{1-7,min}$ and $\Delta T_{1-7,max}$. The two lines end at one point where ΔX reaches the maximum. The points between the two lines represent the system performance for different ΔT_{1-7} between $\Delta T_{1-7,min}$ and $\Delta T_{1-7,max}$.

It is revealed that r and ε increase at a distinctly diminishing rate with the increase of ΔX, and reach the maximum at maximum ΔX. The increase of ΔX is limited by the maximum mass concentration of the strong LiBr–H_2O solution allowed, which is usually taken as 65% as done in this paper (Table 1) because of the sharp increase of the crystallization temperature of the LiBr–H_2O solution at concentrations higher than 65%. Different calculation conditions cause different maxima of ΔX, as shown in Fig. 6 which illustrates the ranges of ΔX and ΔT_{1-7} for different T_{16} and p_1. There is no restriction on the lower limit of ΔX. It is taken as 3% in the analysis, because the r and ε decrease sharply with the decrease of ΔX at lower ΔXs as shown in Fig. 5, and the result is poor system performance for $\Delta X < 3\%$, making the situation seldom used in practice and thus unnecessary to calculate.

Higher ΔX leads to higher water production (Fig. 5), but to a narrower range of ΔT_{1-7} (Fig. 6), indicating the importance of choosing a ΔX suitable for good thermal performance and at the same time offering a certain flexibility in operation and design. It is impossible to give a range or specific suitable values of ΔX, because it changes significantly with calculation assumptions. For instance, with a possible range of ΔX from 3% to 6.15% under $p_1 = 0.25$ MPa and $T_{16} = 70$ °C, the suitable ΔX is around 4%, but when T_{16} is changed to 60 °C, the possible range of ΔX changes to 3%–15%, resulting in a wider suitable range of ΔX from 5% to 9%.

3.2.3. Influence of the motive steam pressure p_1

The motive steam is assumed to be saturated, and Fig. 7 shows the influence of its pressure p_1. With the increase of p_1, the performance ratio r drops slightly, while the exergy efficiency ε drops significantly. To clarify the reasons for this behavior, the exergy utilization of ABHP

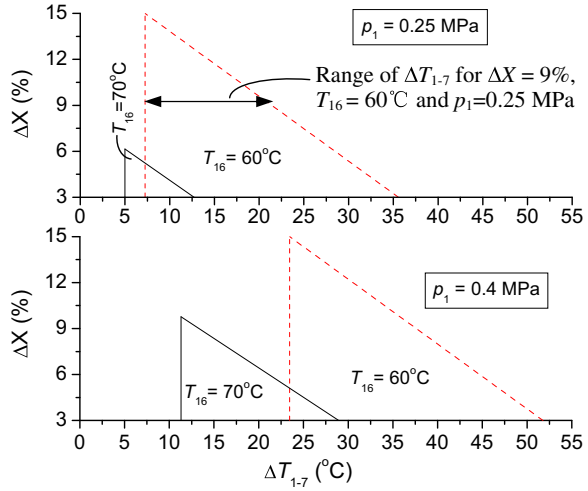

Fig. 6. Ranges of ΔX and ΔT_{1-7} for different T_{16} and p_1.

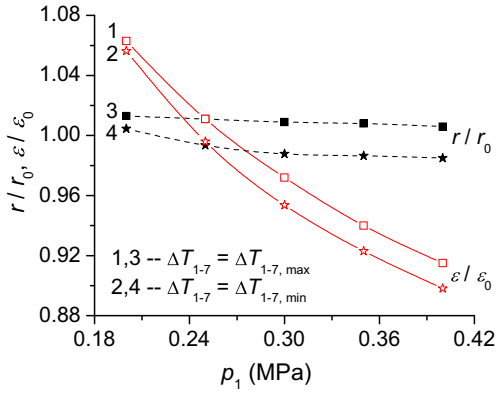

Fig. 7. Effect of p_1 on r and ε for constant T_{16}.

and the thermal energy (exergy), Q_D (E_D), provided by the ABHP to the MEE are calculated for different p_1 and the results are shown in Fig. 8 where ξ_{others} is the sum of the non-dimensional exergy destructions in the solution heat exchanger SH, the flash chamber FC, and in the solution pumps and valves in absorption subsystem. This reveals that the main reason for decreased E_D and then decreased water production is the significant rise of exergy loss in the generator, which is caused by the increased t_1 and consequent enlarged heat-transfer temperature difference with p_1. With the increase of p_1, the thermal exergy input into the ABHP-MEE system by the motive steam increase, while the water production decreases as discussed above, thus causing an obviously decreased ε (Fig. 7).

The above analysis and discussions on the effects of p_1 are performed for a constant T_{16}. A higher p_1 can allow raising of the heating steam (stream 15 in Fig. 1) pressure and correspondingly a higher T_{16}. This, in turn, can allow a higher water production by adding effects to the MEE. For instance, with the maximum ΔT_{1-7} allowed and the other conditions kept constant at the base-case values (Table 1), saturated motive steam of 0.12 MPa can produce heating steam of $T_{16} = 58$ °C at the highest, which is suitable to run a four-effect MEE unit, while motive steam of 0.34 MPa has the ability to produce heating steam of $T_{16} = 72$ °C, suitable to run a seven- or eight-effect MEE unit. More effects lead to a greater potential for producing more fresh water for the same amount of heat input. For instance, increasing T_{16} from 65 °C to 68.4 °C would increase the water production by 14% if the number of effects of the MEE is changed from 6 to 7, without almost any change of the specific heat-transfer area (per kg/s produced fresh water) of the MEE for the two situations. Generally, for the typical range of T_{16} from 58 °C to 72 °C, the ABHP-MEE system analyzed in this paper, which is based on a single-effect absorption heat pump, is applicable to be run by motive steam with p_1 from 0.12 MPa to 0.5 MPa (saturation temperature T_1 from 105 °C to 152 °C).

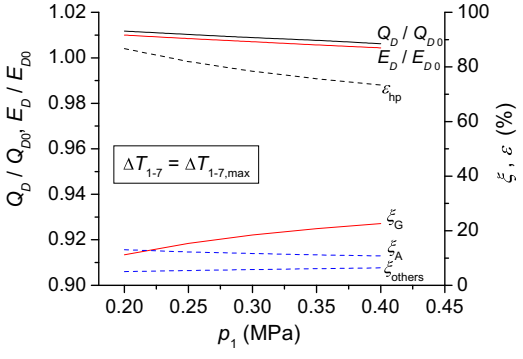

Fig. 8. Performance of ABHP for different p_1 and constant T_{16}.

3.2.4. Influence of the condensation temperature T_{16} of heating steam in the 1st effect

The condensation temperature, T_{16}, of the heating steam in E_1 has a strong effect on the performance of the ABHP-MEE desalination system mainly because (1) T_{16} determines the operating pressure of the generator G, thus influencing the performance of the absorption subsystem and then the parameters of the heating steam supplied to the MEE, and (2) T_{16} is one of the main parameters determining the operating temperature range and then the performance of the MEE.

Fig. 9 shows the normalized thermal energy Q_D and exergy E_D supplied to the MEE, for different values of T_{16}. With the increase of T_{16}, Q_D drops slightly, while E_D rises significantly. Fig. 10 illustrates the exergy utilization of ABHP for $\Delta T_{1-7} = \Delta T_{1-7,max}$ and $T_{16} = 58$ °C, 63 °C and 68 °C. The sum of the exergy destructions in each component and that supplied to the MEE is greater than 100%, about 115% in the three cases in Fig. 10. This is because of the exergy recovery rate λ_R (defined by Eq. (4) and marked in Fig. 10), which is one of the main reasons for the high exergy efficiency of the ABHP. Fig. 10 reveals that the strong increase of E_D with T_{16} is mainly due to the decreased exergy destruction in the generator where the heat-transfer temperature difference has a distinct decrease with increasing T_{16}. Besides increasing the exergy utilization of ABHP, a higher T_{16} also broadens the operating temperature range of the MEE unit, implying the possibility of producing more water by running an MEE with more effects, as discussed in more detail in Section 3.2.3.

3.2.5. Influence of the entrained steam saturation temperature $T_{10,\,sat}$

The influence of the saturation temperature, $T_{10,sat}$ (or pressure p_{10}), of the entrained steam are two-fold. First, a higher $T_{10,sat}$ leads to higher Q_D and E_D (Fig. 11), indicating higher water production. Second, increasing $T_{10,sat}$ narrows the operating temperature range of the MEE, implying a lower water production because of running the MEE with fewer effects when maintaining the heat-transfer temperature difference of each effect the same with that in the base-case conditions. It is thus clear that the effect of $T_{10,sat}$ on water production of ABHP-MEE is determined by the combined action of these two factors.

4. Thermodynamic performance comparison and discussion of ABHP and EHP in desalination processes

The coefficient of performance, COP_{hp}, and the exergy efficiency, ε_{hp}, of ABHP and EHP in desalination processes for different T_{16} are

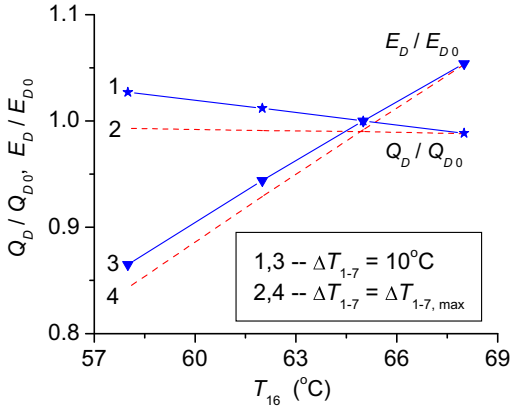

Fig. 9. Q_D and E_D for the MEE for different T_{16}.

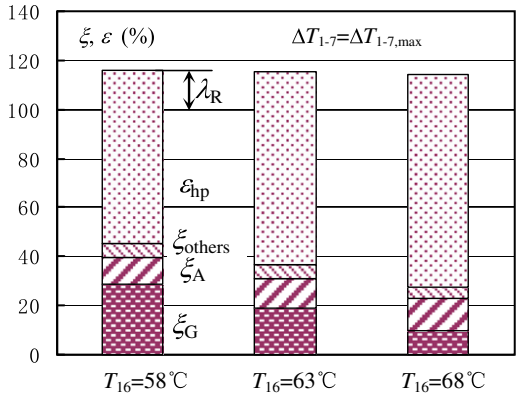

Fig. 10. Exergy utilization of the ABHP for different T_{16}.

calculated, and the results are reported in Fig. 12 for comparison. Lines 2 and 4 in the figure represent the maximum and minimum COP_{hp} and ε_{hp} of ABHP obtained by regulating ΔX and ΔT_{1-7} as discussed in Section 3. The performance of the steam jet ejector was from the empirical correlations in the form of graphs developed by Power [16]. Agreeing with manufacturer's data within the about 10% over the best-fit range, the correlations were generally acknowledged and cited and used by many researchers (cf. [8,17,18]).

It is revealed that for specified p_1 and $T_{10,sat}$, EHP has a higher COP_{hp} and ε_{hp} than ABHP for lower T_{16}, indicating higher water production by EHP-MEE than by ABHP-MEE consuming the same amount of motive steam in this situation. The reason is that for constant $T_{10,sat}$ and then constant p_{10}, decreasing T_{16} leads to the decrease of the compression ratio (the pressure ratio of the heating steam and the entrained steam, p_{16}/p_{10}) of the steam jet ejector, which increases the steam mass flow entrained by per kg/s motive steam according to the performance characteristics of the steam jet ejector [16]. This increases the energy and exergy recovered in the EHP system and results in higher values of COP_{hp} and ε_{hp}, and thus a higher water production. It is thus clear that the commonly held viewpoint [5,19] that ABHP is more energy/exergy-efficient than EHP, or that ABHP-MEE has a higher water production than EHP-MEE, is true only in certain parameter ranges.

The performance of the EHP in desalination processes is determined mainly by the three parameters: p_1, T_{16} and $T_{10,sat}$, while that of the ABHP is determined by more than these three. From Section 3, with specified p_1, T_{16} and $T_{10,sat}$, the minimum and maximum values of COP_{hp} and ε_{hp} of ABHP can be calculated. Within the parameter range studied ($p_1 = 0.12–0.5$ MPa, $T_{16} = 56–72$ °C and $T_{10,sat} = 38–46$ °C), the maxima are up to 6.5% higher than the minima, making it

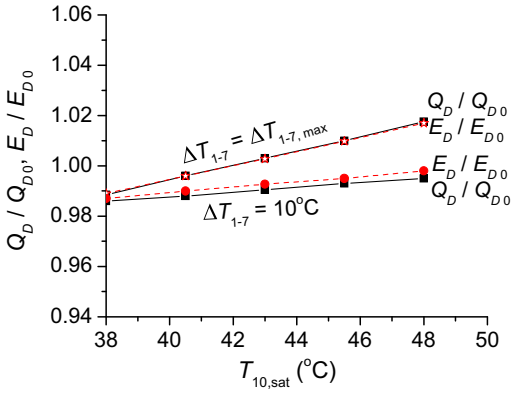

Fig. 11. Effect of $T_{10,sat}$ on system performance.

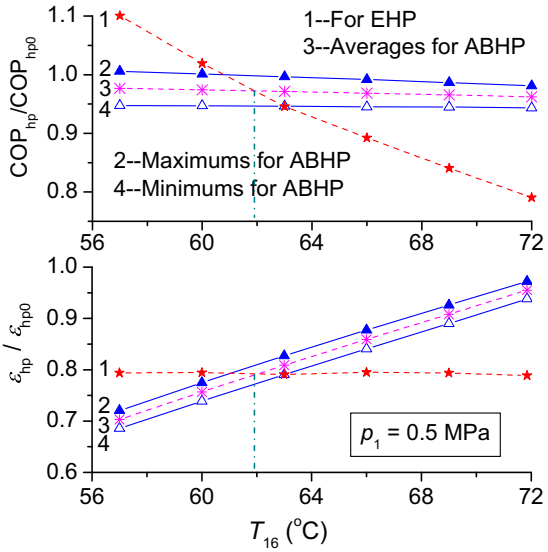

Fig. 12. COP_{hp} and ε_{hp} for ABHP and EHP.

possible to use the mean values to represent approximately the performance of the ABHP (Line 3 in Fig. 12). For a given p_1, one value of $T_{10,sat}$ corresponds to one value of T_{16} at which ABHP and EHP have the same COP_{hp} or ε_{hp}. For example, in Fig. 12 where $p_1 = 0.5$ MPa and $T_{10,sat} = 42$ °C, T_{16} has the value of about 62 °C at the intersection of the performance lines of the two systems. The ABHP has a more favorable thermal performance when $T_{16} > 62$ °C, and conversely, EHP has a more favorable thermal performance when $T_{16} < 62$ °C.

Fig. 13 shows T_{16} against $T_{10,sat}$ for different p_1. Fig. 13 can be used to roughly decide whether ABHP or EHP is the more favorable system thermodynamically, for different conditions. For example, when $p_1 = 0.5$ MPa and $T_{10,sat} = 40$ °C, T_{16} is about 60.1 °C from Fig. 13 (Point A), at which ABHP and EHP have the same energy/exergy performance. The higher the value of T_{16} is than that read from Fig. 13, the more is the ABHP thermally advantageous over EHP, and vice versa (Fig. 12).

5. Economic performance and discussions

Water production cost by the ABHP-MEE is a key factor in determining whether the system is applicable. Owing to the complex influence of the thermodynamic parameters, the material, structure and cost of the components (especially the heat exchangers), the cost of driving energy, etc., on system performance

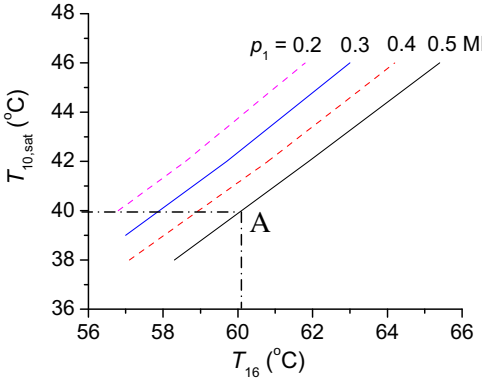

Fig. 13. $T_{10,sat}$ versus T_{16} for different p_1.

and water cost, a complete and thorough economic optimization and analysis of ABHP-MEE remains to be performed. As an initial economic analysis, this section focuses on the compositions of water cost, the economic performance of ABHP and economic comparison of ABHP-MEE and EHP-MEE.

5.1. Economic performance of the base-case system and discussion on ABHP

The evaluation is performed based on the financial condition in China. The exchange rate between US dollar and RMB is taken as 6.83RMB/$. Most of the MEE or EHP-MEE units running or under construction in China are imported. Examining these units and those available in references [20–22], the specific capital cost of MEE plants is found to be $850–1250/ton-product-water/day depending on the manufacturer and production capacities, and here it is thus assumed to be $1000/ton/day. The ABHP subsystem is mainly composed of heat exchangers and pumps, and the capital cost is calculated from the correlations in [23], where the cost is updated with the help of Marshall & Swift Equipment Cost Index [24] and a geographic factor of 0.5 is introduced considering the state-of-the-art technology and the selling price of absorption systems in China. The annual capital cost of MEE or ABHP can be determined by multiplying the capital cost and the amortization factor α,

$$\alpha = \frac{i(i+1)^n}{(1+i)^n - 1} \tag{7}$$

where i is the interest rate and n is the number of years of the economic life of the system, taken as 0.05 and 20, respectively, in the evaluation.

The annual operating cost mainly includes the cost on energy (heat and electricity), seawater-pretreatment chemical, labor, maintenance and management, with the following assumptions made in the evaluation: unit electricity cost is 0.07$/kWh; chemical consumption per ton seawater is 0.005 kg/ton, and unit chemical cost is 1.46$/kg; the yearly operators' salary is $6000/operator with the plant using 12 operating workers; the annual maintenance cost is estimated as 1.5% of the capital cost; the annual management cost is estimated as 20% of the labor cost.

The heat energy cost is the main part of the operating cost, and the unit steam cost y ($/ton) is one of the most important factors determining whether the ABHP based system is economically favorable. y depends significantly on the steam conditions, source, and the cost evaluation method used. Clearly, it is unnecessary to add an ABHP to an MEE if formerly discarded heat is used and when thus y is zero or of very low value. In most situations, however, even low-temperature heat sources come at the expense of the reduction of other useful products, e.g., the generation of such heat in a power-heat cogeneration plant reduces the power production and thus raises the value of y. For instance, based on the equivalent-electricity-consumption cost allocation method [25,26] at which the steam cost is evaluated as the cost of the electricity that the steam can produce in a steam turbine and a generator, the cost of the saturated steam at pressures of 0.25 MPa and 0.5 MPa is $9.6/ton and $11.4/ton, respectively, taking the unit electricity cost as $0.07/kWh.

Table 2 shows the cost data of the base-case system illustrated in Table 1. Since the unit steam cost may change in a very wide range as discussed above, different values, $2/ton, $5/ton, $8/ton and $11/ton, are taken for 0.25 MPa saturated steam to illustrate its influence. Fig. 14 graphically shows the composition of water cost of ABHP-MEE. It is revealed from Table 2 that significant economic benefit can be obtained by adding a steam jet ejector or an ABHP to an MEE when a suitable driving heat source is available. In the base case, the unit water cost decreases by 13.6% and 16.0% respectively, when $y = \$2$/ton, and by 24.3% and 29.7% when $y = \$8$/ton. Clearly, it is more beneficial here to add an ABHP rather than a steam jet ejector to the MEE unit.

Table 2
Summarized cost data for the base-case system.

Water production capacity, ton/day		5,000		
Capital cost of ABHP-MEE, $		5,380,587		
Capital cost of MEE, $		5,000,000		
Capital cost of ABHP, $		380,587		
Annual capital cost of ABHP-MEE,$/y		431,752		
Annual capital cost of MEE, $/y		401,213		
Annual capital cost of ABHP, $/y		30,539		
	$y = \$2$/ton	$y = \$5$/ton	$y = \$8$/ton	$y = \$11$/ton
Annual operating cost of ABHP-MEE, $/y	764,161	1,293,985	1,823,801	2,353,626
Thermal energy cost, $/y	353,215	883,039	1,412,855	1942,680
Electricity cost, $/y		218,453		
Chemical cost, $/y		25,384		
Labor cost, $/y		72,000		
Maintenance cost of MEE, $/y		75,000		
Maintenance cost of ABHP, $/y		5709		
Management cost, $/y		14,400		
Unit capital cost of ABHP-MEE, $/ton		0.249		
Unit capital cost of MEE, $/ton		0.231		
Unit capital cost of ABHP,$/ton		0.018		
Unit operating cost of ABHP-MEE, $/ton	0.441	0.746	1.052	1.357
Thermal energy cost, $/ton	0.204	0.509	0.815	1.120
Electricity cost, $/ton		0.126		
Chemical cost, $/ton		0.015		
Labor cost, $/ton		0.041		
Maintenance cost of MEE, $/ton		0.043		
Maintenance cost of ABHP, $/ton		0.003		
Management cost, $/ton		0.008		
Unit water cost, $/ton				
Unit water cost of MEE, $/ton	0.81	1.33	1.85	2.37
Unit water cost of EHP-MEE, $/ton	0.70	1.05	1.40	1.75
Unit water cost of ABHP-MEE, $/ton	0.68	0.99	1.30	1.61

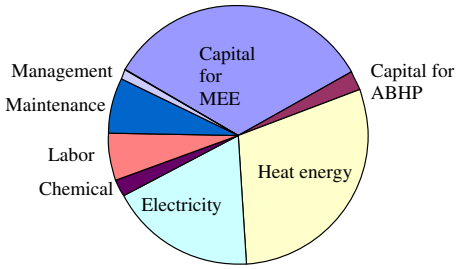

Fig. 14. Composition of the product water cost for the base-case ABHP-MEE system when $y = \$2$/ton.

The MEE technology has been commercialized for many years. Owing to the specified operating parameters of commercially available MEEs, the economic optimization of ABHP-MEE is thus, in most situations, an optimization of just the parameters of the ABHP component. For specified heat source and MEE unit, ΔX and ΔT_{1-7} become important parameters influencing the performance of ABHP and then the water cost of the ABHP-MEE. Fig. 15 shows the unit water cost, c, of ABHP-MEE for different ΔX and ΔT_{1-7} when $y = \$8$/ton, with the other conditions kept constant at the base-case values. c is normalized by its base-case value $c_0 = \$1.30$/ton (Table 2). It is revealed that higher ΔX and ΔT_{1-7} lead to lower c, with the trend verified also by the other calculations performed. Comparing with Figs. 4 and 5 that report the variation of the thermodynamic performance of ABHP-MEE with ΔX and ΔT_{1-7}, we note that the effect of ΔX and ΔT_{1-7} on thermodynamic and economic performance is consistent, that is, higher ΔX and ΔT_{1-7} improve both thermal and economic performance of ABHP-MEE, and v. v. The reason is that, the capital cost of ABHP accounts only for very small part of the water cost, while the thermal energy cost accounts for a big part of that, 2.6% and 29.5%, respectively, in the case shown in Fig. 14 where $y = \$2$/ton, and 1.8% and 51.2%, respectively, when y changes to \$5/ton (Table 2). Calculation results show that although in some situations the capital cost of ABHP increase with ΔX and ΔT_{1-7}, its influence on water cost is negligible; For instance, increasing ΔT_{1-7} from 10 °C at the base case to 15 °C, the capital cost of ABHP increases from \$380,587 to \$397,437, while its contribution to the unit water cost increases only from \$0.0176/ton to \$0.0184/ton), thus making the thermodynamic performance the factor determining the variation of the water cost. We thus conclude that when designing an ABHP for an existing MEE, it is economically favorable to choose ΔX and ΔT_{1-7} to be as high as possible, but considering the discussions in Section 3.2.2, the values should be within suitable ranges to ensure a certain flexibility for plant operation.

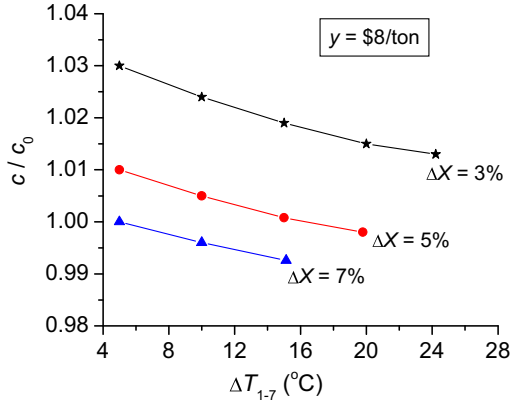

Fig. 15. Effect of ΔX and ΔT_{1-7} on unit water cost of the ABHP-MEE.

5.2. Economic performance comparison of ABHP-MEE and EHP-MEE

The absorption subsystem is clearly more complex and expensive than the steam jet ejector subsystem, the cost of which is nearly negligible relative to the balance of the system. Consequently, for specified heat source conditions and MEE performance at which the EHP has a higher COP_{hp} or ε_{hp} than the ABHP (Fig. 12), and thus the EHP-MEE consumes less driving steam than the ABHP-MEE with the same water production, the economic preference for the EHP-MEE is obvious. The situation becomes more complex for conditions under which the ABHP-MEE consumes less steam per unit produced water than the EHP-MEE.

For ABHP-MEE or EHP-MEE based on the same MEE unit and thus having the same water production capacity, the annual capital and operating costs (excluding thermal energy cost) of the two MEE subsystems, to be called Z, are clearly the same. Neglecting the capital cost of the steam jet ejector, the annual total cost of the EHP-MEE can be expressed as

$$Y_{EHP-MEE} = Z + \frac{y \cdot D \cdot f \cdot 365}{r_{EHP-MEE}} = Z + \frac{y \cdot D \cdot f \cdot 365}{r_{MEE} \cdot COP_{EHP}} \tag{8}$$

where the second term on the right side is the annual heat cost, D is the water production capacity that is assumed to be 5000 ton/day, and f is the plant availability factor here assumed to be 0.95. The annual total cost of the ABHP-MEE can be expressed as

$$Y_{ABHP-MEE} = Z + \frac{y \cdot D \cdot f \cdot 365}{r_{MEE} \cdot COP_{ABHP}} + \alpha C_{ABHP} + 0.015 C_{ABHP} \tag{9}$$

The third term on the right side is the annual capital cost of the ABHP, and the fourth term is the annual maintenance cost of the ABHP here estimated to be 1.5% of the ABHP capital cost. The other operating costs increased by adding the ABHP are neglected owing to their negligible influence on water cost. When $Y_{ABHP\text{-}MEE} < Y_{EHP\text{-}MEE}$, and thus

$$(\alpha + 0.015) C_{ABHP} < \frac{y \cdot D \cdot f \cdot 365}{r_{MEE}} \left(\frac{1}{COP_{EHP}} - \frac{1}{COP_{ABHP}} \right) \tag{10}$$

the ABHP-MEE is more economical than the EHP-MEE, and v.v. The left-side term, that we call Y_{ABHP}, is the annual cost increased by adding the ABHP, and the right side term, that we call Y_s, is the annual thermal energy cost saved owing to the improved COP_{hp} of the ABHP over the EHP. The payback period of the ABHP can be calculated by

$$N = \frac{C_{ABHP}}{Y_s} \tag{11}$$

Fig. 16 shows the Y_{ABHP} and Y_s for the base-case condition (Tables 1 and 2) for different interest rates, which strongly influence Y_{ABHP}, and different unit steam costs, which strongly influence Y_s. The analysis thus shows that Y_s increases linearly with the increase of the unit steam cost y. Y_s is greater than Y_{ABHP}, and thus the ABHP-MEE has better economic performance than the EHP-MEE, only when y is greater than a certain value, \$1.44/ton under $i = 0.05$, and \$2/ton under $i = 0.1$. Fig. 16 also shows that higher y also leads to shorter payback periods of ABHP. For example, N is 3.8 years for $y =$ \$4/ton and 2.5 years for $y =$ \$6/ton.

Fig. 13 in Section 4 can be used to roughly decide whether an ABHP-MEE or EHP-MEE is more favorable thermodynamically, for different conditions. It is almost impossible to produce such a Figure for economic evaluation, owing to the complex influence of more parameters on the economic performance of ABHP-MEE and EHP-MEE.

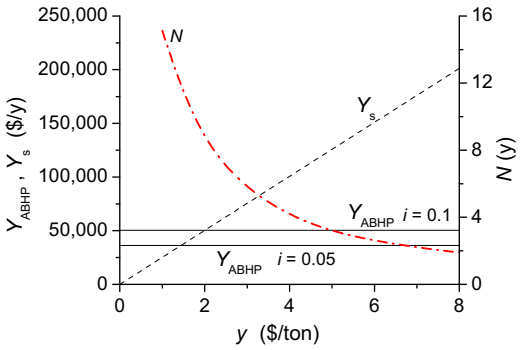

Fig. 16. Variation of Y_{ABHP}, Y_s and N with y for the base-case system.

Based on this study, we recommend the following procedure for economic comparison of ABHP-MEE and EHP-MEE that are integrated with the same MEE unit and use the same heat source conditions: (1) use Fig. 13 to decide whether the ABHP or EHP has a more favorable thermal performance. If EHP does, then the EHP-MEE will definitely be much more economical and should be the choice; if ABHP does, then (2) use Eq. (10) to decide whether ABHP-MEE or EHP-MEE has a more favorable economic performance. If Eq. (10) is satisfied, then a detailed economic analysis is needed to determine how much the economic benefit is and whether it is high enough to support the choice of an ABHP-MEE rather than an EHP-MEE.

6. Conclusions

This study presents a thermal and economic performance analysis of a low-temperature multi-effect evaporation water desalination system (LT-MEE) integrated with a heat-driven single-effect LiBr–H_2O absorption heat pump (ABHP). Owing to the coupling, a 60–78% water production gain over a stand-alone LT-MEE unit run by the same heat source conditions can be obtained within the parameters ranges studied. Typically, driving steam with pressure of 0.12–0.5 MPa is applicable to run the system.

The thermodynamic sensitivity analysis shows that (1) a higher generator approach temperature improves the energy/exergy utilization of the ABHP-MEE system, (2) using driving steam of higher pressure allows increasing the pressure of the heating steam for MEE, and thus increasing the number of effects of the MEE, and consequently producing more water for the same energy input, (3) increasing the strong-and-weak solution concentrations improves the thermal performance of the ABHP-MEE, but narrows the range of the generator approach temperatures, thus reducing the flexibility of system design and operation.

The thermodynamic comparison between ABHP and EHP shows that, the commonly held view that ABHP has more favorable thermal performance than EHP is true only in certain parameters ranges. The parameter ranges were discussed, and a Figure was produced for roughly deciding whether the ABHP-MEE or the EHP-MEE is more favorable thermodynamically, for different conditions.

The economic analysis of ABHP-MEE and the economic comparison between ABHP-MEE and EHP-MEE shows that (1) the capital cost of the ABHP accounts for very small part of the water cost, and when designing an ABHP for an existing MEE unit, the parameters selection of ABHP for lower water cost is consistent with that for better thermal performance, (2) the unit steam cost is an important factor in determining whether the ABHP-MEE or the EHP-MEE is economically favorable; For the conditions under which ABHP-MEE has better thermodynamic performance, only unit steam costs higher than a certain value lead to more economical ABHP-MEE than EHP-MEE. Also, a recommended general economic comparison procedure between ABHP-MEE and EHP-MEE was outlined.

Acknowledgements

The authors gratefully acknowledge the support of the National Natural Science Foundation of China (Project No. 50676023), the Science and Technology Innovation Platform Foundation of Fujian Province, China (Project No. 2009H2006), the Educational Department of Fujian Province, China (Project No. JA10193) and the Foundation for Innovative Research Team of Jimei University, China (Project No. 2009A002).

References

[1] Kronenberg G, Kokiec F. Low-temperature distillation processes in single- and dual-purpose plants. Desalination 2001;136(1–3):189–97.
[2] Darwish MA, Alsairafi A. Technical comparison between TVC/MEB and MSF. Desalination 2004;170(3):223–39.
[3] Alafour FN, Darwish MA, Bin Amer AO. Thermal analysis of METVC + MEE desalination systems. Desalination 2005;174(1):39–61.
[4] Aly SE. A study of a new thermal vapor compression/multi-effect stack (TVC/MES) low temperature distillation system. Desalination 1995;103(3):257–63.
[5] Su J, Han W, Jin H. A new seawater desalination system combined with double-effect absorption heat pump. Journal of Engineering Thermophysics 2008;29(3):377–80 [in Chinese].
[6] Gunzbourg J, Larger D. Cogeneration applied to very high efficiency thermal seawater desalination plants. Desalination 1999;125(1–3):203–8.
[7] Alarcon-Padilla D, Garcia-Rodriguez L, Blanco-Galvez J. Assessment of an absorption heat pump coupled to a multi-effect distillation unit within AQUASOL project. Desalination 2007;212(1–3):303–10.
[8] El-Dessouky HT, Ettouney HM. Fundamentals of salt water desalination. The Netherlands: Elsevier; 2002.
[9] Wang Y, Lior N. Performance analysis of combined humidified gas turbine power generation and multi-effect thermal vapor compression desalination systems—part 1: the desalination unit and its combination with a steam-injected gas turbine power system. Desalination 2006;196(1–3):84–104.
[10] Darwish MA, Al-Asfour F, Al-Najem N. Energy consumption in equivalent work by different desalting methods: case study for Kuwait. Desalination 2002;152(1–3):83–92.
[11] F-chart Software, https://www.fchart.com/ [accessed on 25.02.10].
[12] Kaita Y. Thermodynamic properties of lithium bromide-water solution at high temperatures. International Journal of Refrigeration 2001;24(5):374–90.
[13] Husain A. Integrated power and desalination plants. Oxford, UK: EOLSS publishers; 2003.
[14] Dai Y. Technology and application of lithium bromide absorption refrigeration. Beijing: Mechanical Industry; 2002 [In Chinese].
[15] Wang Y, Lior N. Fuel allocation in a combined steam-injected gas turbine and thermal seawater desalination system. Desalination 2007;214(1–3):306–26.
[16] Power R. Steam jet ejector for the process industries. New York: McGraw Hill; 1994.
[17] Al-Najem NM, Darwish MA, Youssef FA. Thermovapor compression desalters: energy and availability — analysis of single- and multi-effect system. Desalination 1997;110(3):223–38.
[18] Aly NH, Karameldin A, Shamloul NM. Modelling and simulation of steam jet ejector. Desalination 1999;123(1):1–8.
[19] Alarcon-Padilla D, Garcia-Rodriguez L. Application of absorption heat pumps to multi-effect distillation: a case study of solar desalination. Desalination 2007;212(1–3):294–302.
[20] Ran G. Seawater desalination and its application in power plants. Electrical Equipment 2006;7(9):1–5 [in Chinese].
[21] Almulla A, Hamad A, Gadalla M. Integrating hybrid system with existing thermal desalination plants. Desalination 2005;174(2):171–92.
[22] Ophir A, Lokiec F. Review of MED fundamentals and costing, http://www.ide-tech.com/media-center/articles/Review-med-fundamentals-and-costing ([accessed on 25.02.10].
[23] Huang W. Optimization design of thermal equipments and systems. Beijing: Higher Education Press; 1998 [in Chinese].
[24] Plant cost index, http://www.che.com/pci/ [accessed on 25.02.10].
[25] Song Z, Hu S, Zhou S. Indigenous construction of sizeable desalination units for dual-purpose power plants in China. Energy 1991;16(4):721–6.
[26] Zhou S, Hu S. The unified indexes for evaluating the performance of desalination processes. Technology of Water Treatment 2001;27(2):74–9 [in Chinese].